Proc. 14th Int. Conf. Solid-State Sensors, Actuators and Microsystems (Transducers'07), Vol. 2, 2007, Lyon, pp. 863-866.

ELECTROMECHANICAL MODELING OF MICRO ELECTRET GENERATOR FOR ENERGY HARVESTING

Takumi Tsutsumino, Yuji Suzuki, and Nobuhide Kasagi

Department of Mechanical Engineering, The University of Tokyo, Japan
(Tel: +81-3-5841-6419; E-mail: ysuzuki@thtlab.t.u-tokyo.ac.jp)

Abstract: A numerical model for in-plane electret power generators has been developed. Through detailed comparison, we have confirmed that the response of the present model is in good agreement with our experimental power generation data. Electrostatic force both in the horizontal and vertical directions is examined with the model computation. We also propose an electrode arrangement for reducing the in-plane unidirectional damping force. With this arrangement, the damping force of the electret generator becomes similar with that of the velocity-damped resonant generator.

Keywords: Energy harvesting, Electret, Power generator, Model, Electrostatic force

1. INTRODUCTION

Energy harvesting from environmental vibration now attracts much attention in view of its possible applications to RFIDs and automotive sensors [1, 2]. Since the frequency range of vibration existing in the environment is below a few tens of Hz, electret power generators [3,4] should have higher performance than electromagnetic ones. We recently discover that CYTOP, which is MEMS-friendly amorphous perfluoropolymer, can sustain a very-high surface charge density as a stable electret material [5]. We also demonstrate that up to 0.28 mW power can be obtained with an in-plane prototype device at an oscillation frequency as low as 20Hz.

Recently, Mitcheson et al. [6] made analysis of three kinds of power generators; velocity-damped resonant, coulomb-damped resonant, and coulomb-force parametric generators. They show that maximum power output is scaled with $Y_0^2\omega^3 m$, where Y_0, ω, and m respectively correspond to the source motion amplitude, the angular frequency of vibration, and the seismic mass. However, it remains unclear whether the response of in-plane electret generators belongs to one of their models.

In the present study, we develop a computational model of the electret generators, and investigate the damping force during its operation. In addition, we make a coupled simulation of electric circuits and a mechanical system in order to examine its performance under realistic vibration condition.

2. IN-PLANE ELECTRET POWER GENERATOR

Figure 1 shows a schematic of the micro electret generator proposed in the present study. When vibration in the in-plane direction is applied, the seismic mass undergoes a relative motion with respect to the substrate. The amount of the induced charge on the counter electrode is changed due to the change in the overlapping area between the electret and the counter electrode, producing an alternative electric current in the external circuit. The seismic mass is supported by parylene high-aspect-ratio springs [7, 8], which enable large-amplitude oscillation and low resonance frequency. Advantage of the in-plane configuration rather than the out-of-plane counterpart is that the amplitude can be large, while the gap between the electret and the counter electrode is kept small, which results in large power output.

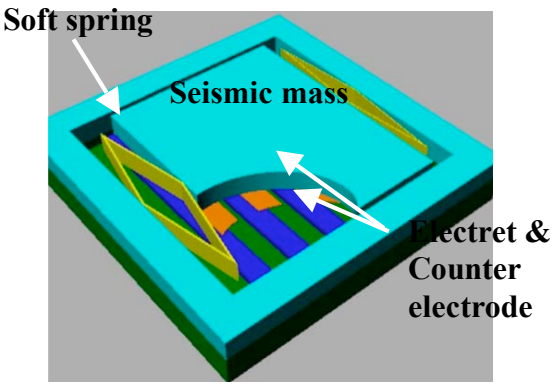

Figure 1: Micro electret generator

3. NUMERICAL MODEL OF ELECTRET GENERATOR

Figure 2 shows a computational model of the generator, where σ, d, and g are respectively the surface charge density, thickness of the electret film, and the gap between the electret and the counter electrode. The interdigital electrodes consist of base/counter electrodes and guard electrodes. The length x_1 represents the overlapping area between the electret film and the counter electrode. The parasitic capacitance C_p is assumed to be constant as described later.

One-dimensional electrostatic field is assumed in the present study. Applying Gauss's law at the electret surface, we get

$$-\varepsilon\,\varepsilon_0 E_b + \varepsilon_0 E_a = \sigma, \qquad (1)$$

where E_b, E_a, and ε are respectively electrostatic fields in the electret film and the air gap, and relative permittivity of the electret material. With the Kirchhoff's law, we get

$$V + dE_b + g\,E_a = 0, \qquad (2)$$

and

$$V + (d+g)E_c = 0, \qquad (3)$$

where V and E_c are respectively the output voltage and the electrostatic field between the counter electrode and the guard electrode.

The induction current $I(t)$ is given by the conservation of charge :

$$\sigma_{i1} b x_1 + \sigma_{i2} b x_2 + \int_0^t I(t)dt = Q\ (\text{const.}), \qquad (4)$$

where σ_{i1} and σ_{i2} are the induced charges on the counter electrode, which are respectively given by

$$\sigma_{i1} = -\varepsilon_0 E_a, \text{ and } \sigma_{i2} = -\varepsilon_0 E_c. \qquad (5)$$

The quantity b represents the length of the electrodes.

Substituting Eqs. (1-3, 5) into Eq. (4), a differential equation with respect to the output voltage $V(t)$ is obtained. We employ numerical analysis to solve Eqs. (1-5), since they have no analytical solution unlike more simplified form given by Tada [3].

For real applications, rectification, smoothing and charging circuits, which show nonlinear behaviors, are connected to the generator. In the present study, a resistance R is assumed for simplicity.

Electrostatic damping force is examined as follows: Considering the conservation of energy, the work done by the external force $F_x dx/dt$, power consumption at the load resistance V^2/R and the electrostatic potential energy E_s satisfy

$$\frac{dE_s}{dt} + \left\{\frac{V^2}{R} + C_p V \frac{dV}{dt}\right\} + F_x \frac{dx}{dt} = 0, \qquad (6)$$

where F_x is the force in the horizontal direction needed for the prescribed oscillation amplitude. The electrostatic energy E_s can be computed with E_a, E_b, and E_c. Since the parasitic capacitance in the actual experimental setup is unknown, we estimate its value with a least square fit to the experimental data.

Figure 3 and Table. 1 shows the experimental setup [5] and the experimental

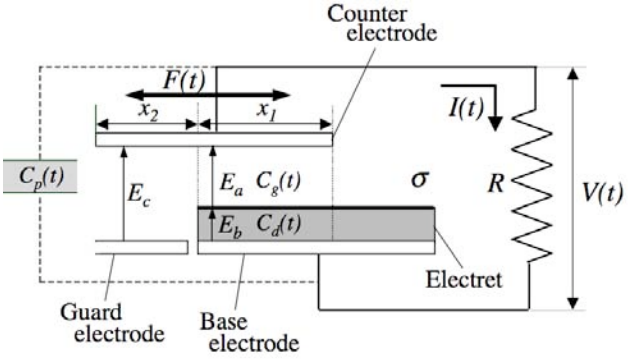

Figure 2: Computational model of electret generator

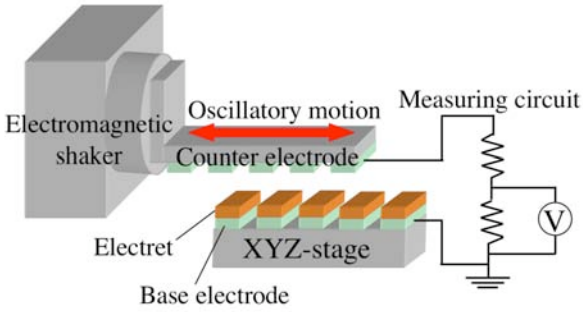

Figure 3: Experimental setup for power generation [5].

Table 1. Experimental condition [5].

Electrode width	150 μm
Gap between top and bottom plates	40 μm
Electret thickness	20 μm
Surface potential	-600 V
Oscillation frequency	20 Hz
Oscillation amlitude	1.2 mm_{p-p}
Maximum power	0.278 mW

conditions. In our experiment, the electret plate and the counter electrode plate are respectively fixed to an electromagnetic shaker and an alignment stage. The counter electrode plate is moved sinusoidally in the in-plane direction by the shaker. The distance between the top and bottom glass substrates is set to 40 μm. The gap between the electret surface and the counter electrode is 20 μm, and the theoretical capacitance for the 100 % overlap is 88.5 pF. The surface potential of the electret film is -600 V. Oscillation frequency and amplitude are respectively 20 Hz and 1.2 mm_{p-p}.

4. COMPUTATIONAL RESULTS

Figure 4 shows the output power versus the external load R. In our experiment, maximum output power of 0.278 mW is obtained at $R = 4$ MΩ. The simulation results are in good agreement with the experimental data. Figure 5 shows the time trace of the output voltage obtained with $R = 4$ MΩ. Since the amplitude is 8 times larger than electrode width, the output voltage has oscillations at 160 Hz. The peak-to-peak voltage is as large as 120 V. Again, the present simulation results are in good agreement with the experimental data.

It is now clear that the present model can mimic the response of the electret generator with sufficient accuracy. Figure 6 shows the computational results of the electrostatic force acting in the in-plane (horizontal) direction together with the oscillation velocity during one cycle of the sinusoidal movement. It is found that large force of ~0.15 N appears alternatively in opposite directions. The force is in the direction where the overlapping area should increase, and

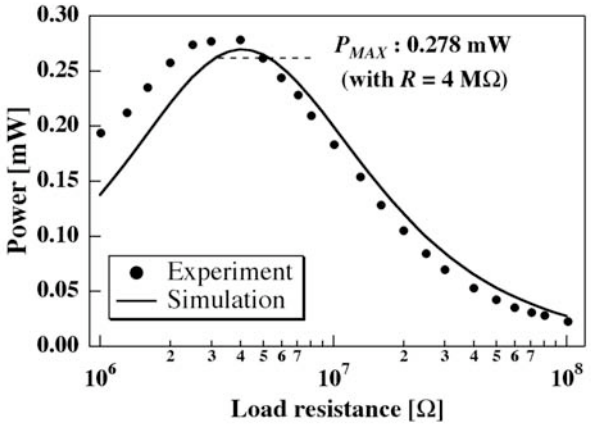

Figure 4: Power output versus external load.

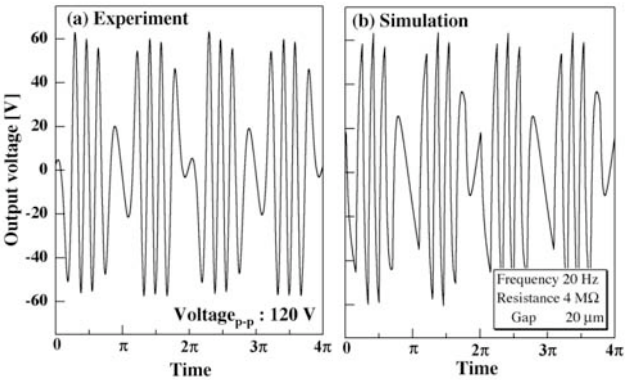

Figure 5: Time trace of the output voltage.

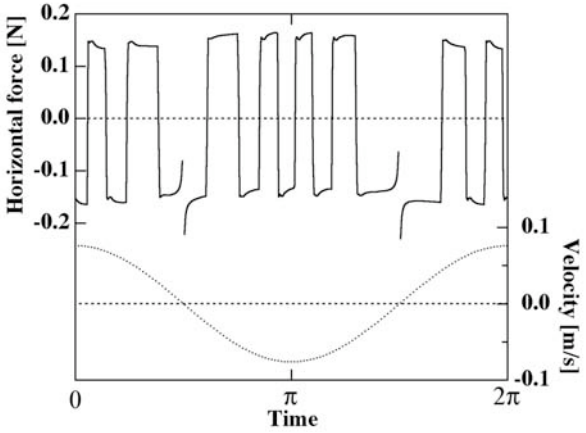

Figure 6: Horizontal electrostatic force for original electrode arrangement.

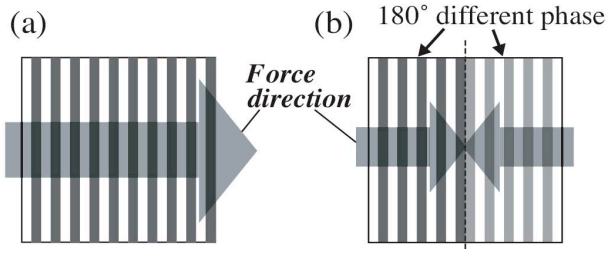

Figure 7: Electrode arrangement. a)Single-phase, b) Two-phase arrangement.

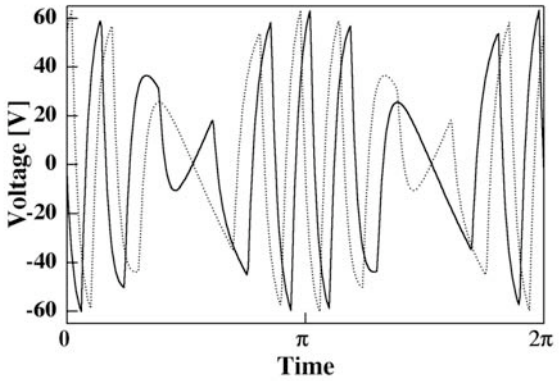

Figure 8: Voltage output for the modified electrode arrangement depicted in Fig. 7b. Solid and dotted lines correspond to the two voltage phases.

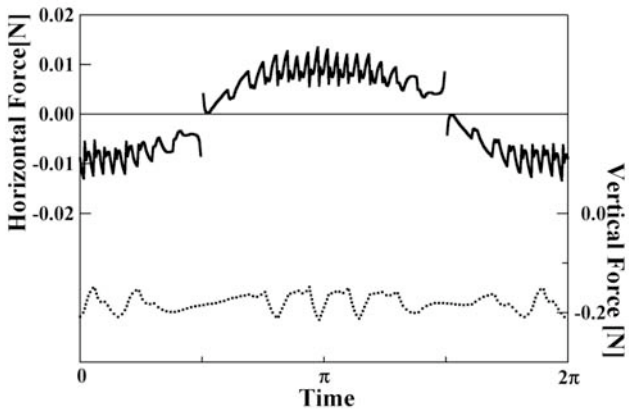

Figure 9: Electrostatic force for the modified electrode arrangement.

switched every time when the poles of the counter electrode pass through the electret poles.

In order to reduce this large horizontal electrostatic force, a modified electrode arrangement, where two electrically-independent generators with an 180˚ phase difference are integrated on a single chip, is proposed as shown in Fig. 7. Figure 8 shows the two phases of the voltage output, which are also 180˚ out-of-phase. Figure 9 shows the horizontal force for the modified electrode arrangement. Large horizontal force shown in Fig. 6 is almost cancelled out, and relatively-small force of about 0.01 N is left. Note that the horizontal force thus obtained is roughly proportional to the velocity, and exhibits similar trends with the velocity-damped resonant generaotor [6]. On the other hand, in the vertical direction, almost constant attraction force of ~0.2 N acts independently of the electrode motion. This is because the surface potential of the electret film is much higher than the time-varying voltage of the counter electrode. Therefore, mechanisms for keeping the gap between the electret and the counter electrode under this large electrostatic attraction force should be crucial to develop high-performance in-plane electret generators.

5. CONCLUSION

We develop a computational model of in-plane electret generators, and evaluate the electrostatic force during their operation. The following conclusions can be derived:

(1) The present generator model can mimic the response of the in-plane electret generator with sufficient accuracy.

(2) When two separate generators with an 180˚ phase difference are integrated on a single chip, the in-plane electrostatic force becomes much smaller. The trend of the in-plane force is similar with that of the velocity-damped resonant model.

(3) Strong vertical attraction force acts between the electret and the counter electrode. Mechanisms for keeping the gap between them under this large electrostatic force should be crucial to realize high-performance in-plane electret generators.

This work is supported through the New Energy and Industrial Technology Development Organization (NEDO) of Japan.

REFERENCE

[1] J. A. Paradiso, and T. Starner, " Energy scavenging for mobile and wireless electronics," IEEE Pervasive Comput., Vol. 4, pp. 18-27, 2005

[2] S. Roundy, P. K. Wright, and J. Rabaey,"A study of low level vibration as a power source for wireless sensor nodes," Comp. Commu., Vol. 26, pp. 1131-1144, 2003.

[3] Y. Tada, " Theretical characteristics of generalized electret generator using polymer film electrets," IEEE Trans. Electrical Insul., Vol. 21, pp. 457-464, 1986.

[4] J. Boland, C.-H. Chao, Y. Suzuki, and Y.-C. Tai,"Micro electret power generator," Proc. 16th IEEE Int. Conf. MEMS, Kyoto, pp. 538-541, 2003.

[5] T. Tsutsumino, Y. Suzuki, N. Kasagi, and Y. Sakane, " Seismic power generator using high-performance polymer electret," IEEE Int. Conf. MEMS 2006, Istanbul, pp. 98-101, 2006.

[6] P. D. Mitcheson, T. C. Green, E. M.Yeatman, and A. S.Holmes, " Architectures for vibration-driven micropower generators," J. MEMS, Vol. 13, pp. 429-440, 2003.

[7] Y. Suzuki, and Y.-C. Tai, " Micromachined high-aspect-ratio parylene spring and its application to low-frequency accelerometer," J. MEMS, Vol. 15, pp. 1364-1370, 2006.

[8] T. Tsutsumino, Y. Suzuki, N. Kasagi, and Y. Sakane, "Nano-metal ink based electrode embedded in parylene structures with the aid of the capillary effect," Proc. IEEE Int. Conf. MEMS 2007, Kobe, (2007), pp. 313-316.